

Synthesis and characterization study of dual phase mixed zinc cobalt ferrite nanoparticles prepared via chemical co-precipitation method

Rohit R. Powar¹, Ashok B. Gadkari², Pravina B. Piste³, Dnyandevo N. Zambare^{1*}

¹Department of Chemistry, Kisanveer Mahavidyalaya, Wai 412803, (MS) India

²Department of Physics, GKG College, Kolhapur 416012, (MS) India

³Department of Chemistry, YCIS, Satara 415001, (MS) India

*Corresponding author

DOI: 10.5185/amp.2018/6997

www.vbripress.com/amp

Abstract

Nanoparticles of Zinc substituted Cobalt ferrite powders having general formula $Zn_xCo_{1-x}Fe_2O_4$ ($x = 0, 0.25, 0.5, 0.75, 1.0$) have been produced by using analytical grade nitrates and hexadecyltrimethylammonium bromide (CTAB) as structure directing reagent via Chemical co-precipitation method. The structure and morphology of prepared polycrystalline ferrite nanoparticles were investigated by X-ray diffraction (XRD), Fourier Transform Infrared Radiation (FTIR) and Scanning electron microscopy (SEM) respectively. Thermogravimetric differential analysis (TG/DTA) technique gives information about ferrite phase formation occurs beyond 450 °C. The XRD analysis confirms the establishment of the cubic spinel structure with the presence of minor secondary phase of $\alpha-Fe_2O_3$ (hematite) at a calcination temperature of 650 °C. The polycrystalline mixed zinc cobalt ferrite nanoparticles showed a dual phase and crystallite size lies in the range 6-11 nm. FE-SEM microstructure shows the nearly spherical polycrystalline nanoparticles with a particle size in between 0.11-0.20 μm . The FT-IR spectra display two significant strong absorption bands nearby in the range of 400 cm^{-1} and 600 cm^{-1} on the tetrahedral and octahedral sites respectively. Copyright © 2018 VBRI Press.

Keywords: Chemical synthesis, nanostructures, XRD, FE-SEM.

Introduction

The polycrystalline ferrite nanoparticles have been interesting materials studied in the earlier decades owed to their uncommon physical, chemical and magnetic properties of nanomaterial with control size, composition and morphology were unlike from the bulk phase properties of materials. Hence researchers are very keen to find the simple, economical and effective method to prepared nanomaterial's having larger surface area. The spinel ferrite fascinates research importance because of their multipurpose practical applications [1]. Ferrite Nanomagnetic material results in numerous applications in heterogeneous catalysis, microelectronic circuits, adsorption, sensors, piezoelectric devices, magnets, magnetic drug delivery [2-8]. Generally, spinel ferrites having MeB_2O_4 structure, where Me is a metal with +2 valence and B are trivalent ferric (Fe^{3+}) cations respectively [9]. Thus unoccupied interstitial sites of large portion were vacant to migrate cations among interstitial sites. The structural, elemental composition and various cations distribution between the tetrahedral (A) and octahedral (B) sites depended on preparation method and sintering temperature. Recently, spinel ferrite nanoparticles were prepared using numerous methods like co-precipitation [10], microwave refluxing [11],

reverse micelle method [12], hydrothermal method [13], sol-gel method [14], spray pyrolysis [15], ceramic method [16] etc.

In this paper, we explosion the synthesis, structural and morphological properties of zinc-substituted cobalt ferrite with general formula $Zn_xCo_{1-x}Fe_2O_4$ ($x = 0-1$). The spinel ferrites were produced via chemical co-precipitation method followed by calcination in the air has several advantages such as simple, good chemical homogeneity and economical method to produce the large quantity of smaller particles and lower sintering temperature as compared to the ceramic method.

Experimental

Material

Polycrystalline zinc substituted cobalt ferrite nanoparticles were synthesized by using the precursor materials as cobalt nitrate hexahydrate ($Co(NO_3)_2 \cdot 6H_2O$), Iron nitrate nonahydrate ($Fe(NO_3)_3 \cdot 9H_2O$), zinc nitrate hexahydrate ($Zn(NO_3)_2 \cdot 6H_2O$), n-hexadecyltrimethylammonium bromide (CTAB), 30 % aqueous ammonia etc. All analytical grade chemical were used as received, without further purification.

Synthesis

The polycrystalline spinel ferrites $Zn_xCo_{1-x}Fe_2O_4$ ($x = 0.0 - 1.0$) nanoparticles were produced by using a chemical co-precipitation method. Cobalt nitrate, zinc nitrate, iron nitrate and CTAB were used as precursor materials. An initial molar proportion of salts cobalt nitrate hexahydrate, zinc nitrate hexahydrate, Iron nitrate nonahydrate were dissolved in minimum quantity of deionized water. An aqueous solution of n-hexadecyltrimethylammonium bromide (critical micelle concentration) was mixed with metal nitrate solution and stirred at 35 °C for 1 h on a hot plate with slow and constant stirring by using a magnetic stirrer. The mixture was then mixed with 30 % aqueous ammonia solution by dropwise addition to getting a dark brown precipitate of metal hydroxide at pH = 9-10. The pH was maintained by dropwise addition of 0.1 N Nitric acid (HNO_3). The precipitate was digested on a hot plate at 80 °C for 2 h. The precipitate was then filtered and washed with ethanol and deionized water followed by drying at 110 °C temperature for 24 h in air. The synthesized powder was milled with acetone in an agate mortar for 1 h. The air-dried powder was then pre-sintered into Muffle furnace at 300 °C for 2 h. Air Cooled powder was again milled in an agate mortar to make the homogenous mixture and finally sintered at 650 °C for 3 h into muffle furnace. The powder was cooled in air and milled in an agate mortar to get a floppy powder.

Characterization

The thermal character of the as-prepared ferrite powder was monitored by TG/DTA (Nietzsche STA 409 TG DSE) instrument with the sample heated from temperature 25 °C to 1000 °C under synthetic air at 10 °C/min heating rate. X-ray powder diffraction investigation was conducted on a PW-1710 Philips X-ray diffractometer (XRD) using $Cu K\alpha$ ($\lambda=1.5406 \text{ \AA}$) radiation. Fourier-transformed infrared (FT-IR) transmission spectra of samples in the range of 800-400 cm^{-1} were recorded using Perkin-Elmer spectrum one spectrophotometer. The surface morphology of the samples was observed by scanning electron microscopy (SEM) using the JEOL JSM 6360 model with magnification range x50 to 100,000.

Results and discussion

Thermo-gravimetric analysis

Thermal behavior and phase formation temperature of spinel ferrites were monitored by thermogravimetric-differential thermal (TG-DTA) analysis. The as-prepared sample $Zn_xCo_{1-x}Fe_2O_4$ ($x = 0.5$) was investigated by TG-DTA analysis. The Fig. 1 shows an initial weight loss step (15.48 %) between temperature range 25 - 180 °C. The second significant weight loss step (8.08 %) around temperature range in between 210 - 350 °C. No further weight loss was observed beyond 450 °C and up to 1000 °C. The weight loss due to loss

of adsorbed moisture and due to the decomposition of the organic matrix also a conversion of metal hydroxides into metal oxides. On the DTA curve, the main exothermic peak was observed at near 270 °C suggesting that combustion of the organic matrix. The plateau formed between 450 °C and 1000 °C on the TG curve indicates the formation of crystalline ferrite.

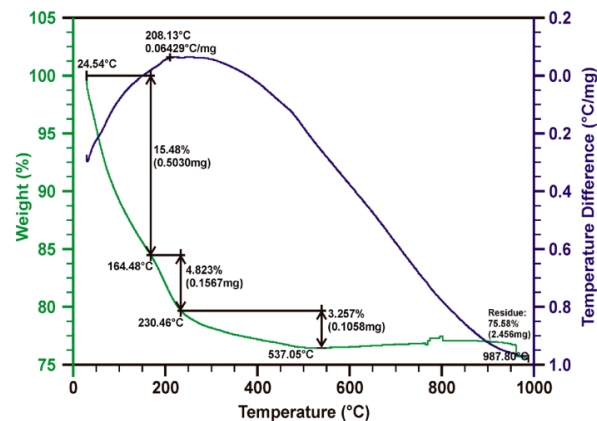


Fig. 1. Thermogravimetric differential analysis curve of as prepared $Zn_{0.5}Co_{0.5}Fe_2O_4$.

X-ray diffraction analysis

The XRD study was done to confirm the structure and secondary phase of the polycrystalline nanoparticles. The XRD pattern of the chemical co-precipitated samples $Zn_xCo_{1-x}Fe_2O_4$ ($x = 0, 0.25, 0.5, 0.75$ and 1) were sintered at 650 °C was shown in Fig 2. The main diffraction peaks were indexed as (220), (311), (222), (400), (422), (511) and (440) which are features of single-phase cubic spinel structure. Peak corresponds to $\alpha-Fe_2O_3$ (hematite) marked as an asterisk (*) were present as a dual phase [17]. The XRD approves the growth of cubic spinel structure in all the samples with minor impurity phase. The X-ray diffraction arrangements agree with JCPDS card number. 77-0011 ($ZnFe_2O_4$) [18] and 22-1086($CoFe_2O_4$) [19].

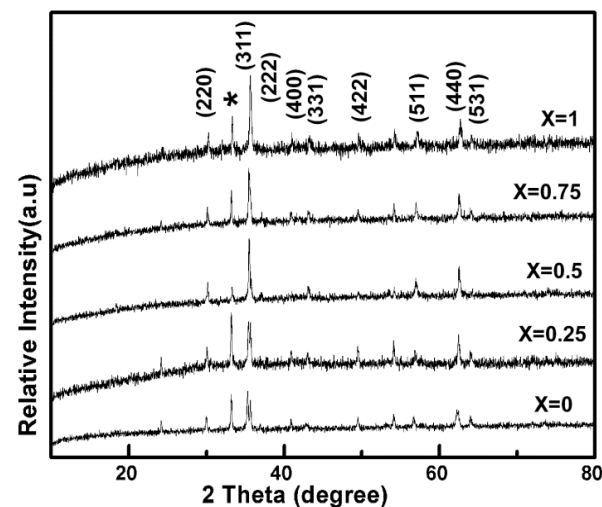


Fig. 2. XRD pattern of $Zn_xCo_{1-x}Fe_2O_4$ ($x = 0, 0.25, 0.5, 0.75$ and 1) Sintered at 650 °C.

The lattice constant of synthesized polycrystalline ferrites nanomaterial was calculated by using the Bragg's equation [20].

$$a = d(h^2 + k^2 + l^2)^{1/2} \tag{1}$$

where h, k, and l are Miller indices of crystal planes. It was apparent that the lattice constant for $Zn_xCo_{1-x}Fe_2O_4$ ($x = 0, 0.25, 0.5, 0.75$ and 1) samples rises with increasing zinc substitution. This occurs due to the exchange of Co^{2+} ions with Zn^{2+} ions. This is also reported by Vaidyanathan *et.al.* [21]. that lattice constant rises with Zn concentration. Polycrystalline ferrite samples average crystallite size was calculated by using the Debye- Scherer equation [22].

$$D = \frac{0.89\lambda}{\beta \cos \theta} \tag{2}$$

where D is the average crystallite size of the ferrite, λ is the incident X-ray wavelength of Cu K α radiation, β is the full-width half maximum (FWHM) in radians in the 2θ scale and θ is the Bragg's angle in radian. The average crystallite size and lattice constant of mixed zinc cobalt ferrite were varied with zinc concentration represented in **Table 1**.

Table 1. Influence of zinc concentration (x) on structural parameters of $Zn_xCo_{1-x}Fe_2O_4$ ($0 \leq x \leq 1$).

Composition (x)	Lattice constant 'a' (Å)	Crystallite size 'D' (nm)	Absorption band (cm ⁻¹)	
			ν_1	ν_2
0	8.3610	6.03	545	415
0.25	8.3915	7.10	541	418
0.5	8.3958	7.89	538	421
0.75	8.3989	9.40	525	425
1	8.4202	10.54	520	428

Fourier transformed infrared study

The FTIR spectrum is one of the methods gives the structural information used to confirm the tetrahedral and octahedral sites of spinel ferrite structure. It also confirms the impurity states and chemical substances adsorbed on the surface of particles. It is observed from **Fig. 3** that the FT-IR spectrum shows two characteristics absorption bands in the range 400-800 cm^{-1} [23]. The higher absorption band wave number ν_1 and lower absorption band wave number ν_2 observed in the range of 545-520 cm^{-1} and 415-428 cm^{-1} respectively. The absorption band at 415 cm^{-1} was for octahedral sites and 545 cm^{-1} was for tetrahedral sites of cobalt ferrite spinel structure. The band observed at around 520 cm^{-1} for $ZnFe_2O_4$ can be assigned to tetrahedral Zn^{2+} stretching ν_1 and the band observed at 428 cm^{-1} involves the Fe^{3+} vibration at the octahedral site ν_2 . Due to the higher weight of zinc, as Zn concentration increases ν_1 is decreasing from

545 cm^{-1} for $CoFe_2O_4$ to 520 cm^{-1} for $ZnFe_2O_4$ were depicted in **Table 1** [24].

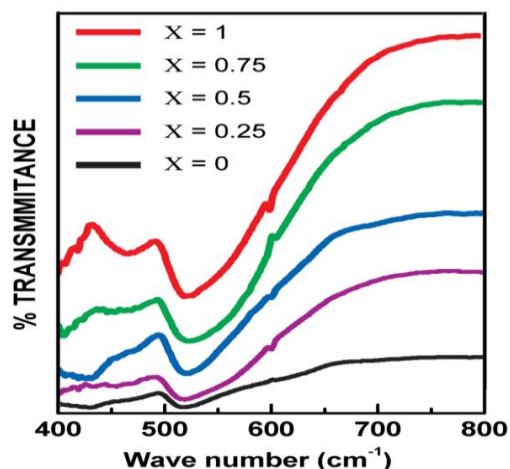


Fig. 3. Infrared absorption spectra of $Zn_xCo_{1-x}Fe_2O_4$ ($x = 0, 0.25, 0.5, 0.75$ and 1).

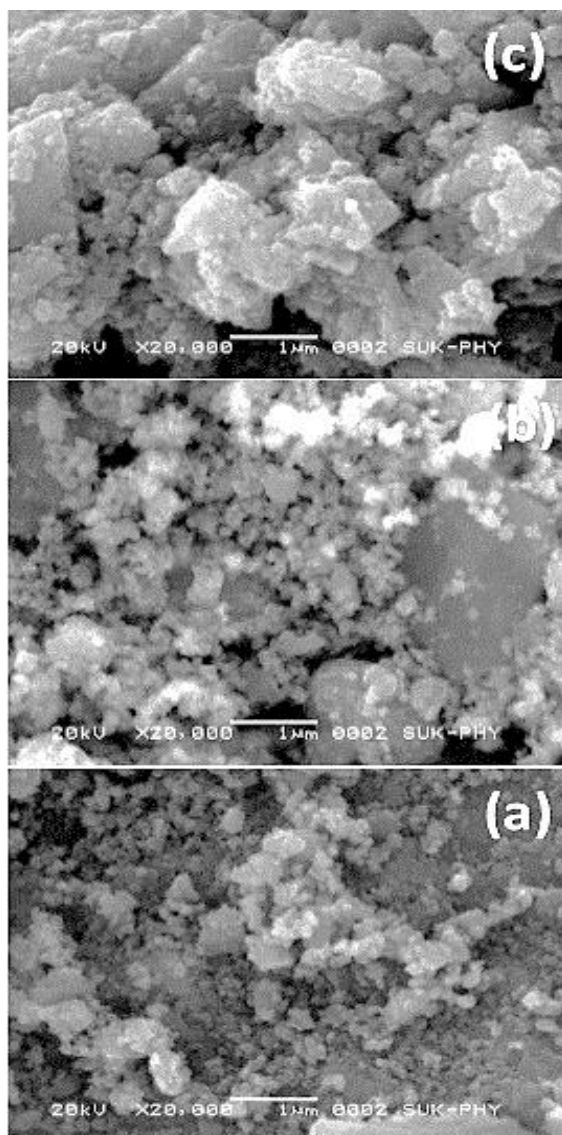


Fig. 4. FE-SEM micrograph of $Zn_xCo_{1-x}Fe_2O_4$ (a) $x = 0$, (b) $x = 0.5$, (c) $x = 1.0$.

Field-emission scanning electron microscopy study

FE-SEM micrographs of the samples $Zn_xCo_{1-x}Fe_2O_4$ ($x = 0, 0.5$ and 1.0) sintered at $650\text{ }^\circ\text{C}$ are shown in **Fig. 4**. The morphological structures of polycrystalline ferrites with nearly spherical shape and size of the particles are almost uniform and agglomerated. The surface of the ferrite powders shows pores formed by the escaping gases during the sintering of powder. The average grain size in the sample calculated by the linear intercept method [25]. The size of grain ranges from $0.11 - 0.20\text{ }\mu\text{m}$. These particles possess voids and pores which helps to grind and obtain fine particles [26].

Conclusion

The polycrystalline zinc substituted cobalt ferrite nanoparticles was successfully synthesized via a chemical co-precipitation method. The face-centered cubic spinel structure of $Zn_xCo_{1-x}Fe_2O_4$ ($x = 0.0, 0.25, 0.5, 0.75$ and 1) with dual phase of $\alpha\text{-Fe}_2\text{O}_3$ (hematite) was observed. The thermogravimetric analysis of the as-prepared sample gives information that above $450\text{ }^\circ\text{C}$ the stable phase of mixed zinc cobalt ferrite nanoparticles was obtained. It has been confirmed by the XRD analysis that impurity phase still present in all spinel ferrite sample sintered at $650\text{ }^\circ\text{C}$ and therefore single cubic spinel phase will be formed at the higher sintering temperature. FT-IR confirms two absorption bands in the range of $400 - 600\text{ cm}^{-1}$. The scanning electron micrograph revealed that all samples were porous network powder and nearly spherical structure.

References

1. Sugimoto, M.; *J. Am. Ceram. Soc.*, **1999**, 82, 269.
2. P.P. Hankare.; P.D. Kamble; S.P. Maradur; M.R. Kadam.; U.B. Sankpal.; K.P. Patil.; K. Nimat.; P.D. Lokhande.; *J. Alloys. Compd.*, **2009**, 487, 730.
3. J. Smit.; *Magnetic Properties of Materials; in: Intra – University Electronics Series.* **1971**, 89.
4. Vasambekar, P.N.; Kolekar, C.B.; Vaingankar, A. S.; *Mater. Res. Bull.* **1999**, 34, (6), 863.
5. T, Mathew.; K, Sree Kumar.; B, S, Rao.; C, S, Gopinath.; *J. Catal.* **2002**, 210, 405.
6. Patange, J.M.; Shirsath, S. E.; Lohar, K.S.; Jadhav, S.S.; Mane, D.R.; Jadhav, K.M.; *J. Mater. Lett.*; **2010**, 64(6), 722.
7. M. H. Sousa.; F. Atourinho.; J. Depeyrot.; G. J. da Silva.; M. C. Lara.; *J. Phys. Chem. B.*; **2001**, 105, 1168.
8. Sudimack, J, B, A.; Lee, R, J.; *Adv. Drug. Deliv. Rev.*; **2000**, 41, 147.
9. J. Smith.; H. P. J. Wijin.; Ferrite. *John Wiley and Sons, New York* **1999**.
10. A.B. Gadkari.; T.J. Shinde.; P.N. Vasambekar.; *J. of Alloys and Compounds*, **2011**, 509, 966.
11. J. Giri., T. Sriharsha.; D. Bhadur.; *J. Mater. Chem.* **2004**, 14, 875.
12. V. L. Calero-Ddelc, C.; Rinaldi.; *J. Magn. Magn. Mater.* **2007**, 314, 60.
13. K, Madhusudan, Reddy.; L, Satyanarayana.; Sunkara, V, Manorama.; R. D. K. Misra.; *Materials Research Bulletin.* **2004**, 39, 1491.
14. P. P. Hankare.; K.R. Sandi.; K.M. Garadkar.; D.R. Patil.; I. S. Mulla.; *J. Alloys Compd.* **2013**, 553, 383.
15. S.Z. Zhang.; G.L. Messing.; *J. Am. Ceram. Soc.* **1990**, 73, 61.
16. S.P. Dalwai.; A.B. Gadkari.; T.J. Shinde.; P.N. Vasambekar.; *Adv. Mat. Lett.* **2013**, 4(7), 586.
17. E. R. Kumar.; P. S. Prasada Reddy.; G.S. Devi.; S. Sathiyaraj.; *J. Magn. Mag. Mater.* **2016**, 398, 281.
18. R. Rameshbabu.; R. Ramesh.; S. Kanagesan.; A. Karthigeyan.; S. Ponnusamy.; *J Mater Sci: Mater Electron.* **2014**, 25, 2583.
19. M. Mozaffari.; S. Manouchehri.; M. H. Yousefi.; J, Amighian.; *J. Magn. Magn. Mater.* **2010**, 322, 383.
20. B.D. Cullity.; *Elements of X-ray diffraction, Addison Wesley Pub Co INC*, **1956**.
21. R. Arulmurugan.; B. Jeyadevan.; G. Vaidyanathan.; S. Sendhilnathan.; *J. Magn. Magn. Mater.*, **2005**, 288, 470.
22. Lawrence, Kumar; Manoranjan, Kar.; *Ceramic international.* **2012**, 38, 4771.
23. R.D. Waldron.; *Infrared spectra of ferrites, Phys. Rev.* **1955**, 99, 1727.
24. F. Gozuak.; Y. Koseoglu.; A. Baykal.; H. Kavas.; *J. Magn. Magn. Mater.* **2009**, 321, 2170.
25. J.C. Warst.; J.A. Nelson.; *J. Am. Ceram. Soc.* **1972**, 55, 109.
26. Y. Zhang.; G.C. Stangle.; *J. Mater. Res.* **1994**, 9, 1997.